# Max-Planck-Institut für Mathematik in den Naturwissenschaften Leipzig

An Analytical Framework For Modeling Evoked and Event-Related Potentials

by

 $Axel\ Hutt$ 

Preprint no.: 46 2002



#### An Analytical Framework For Modeling Evoked and Event-Related Potentials

#### Axel Hutt

Max Planck-Institute for Mathematics in the Sciences Inselstr.22-26, 04103 Leipzig, Germany; email: ahutt@mis.mpg.de

#### Abstract

The presented work introduces shortly a novel segmentation method and a modeling approach for multivariate quasi-stationary data. The combination of both allows the extraction of low-dimensional models from multi-dimensional data. The segmentation method is applied both to event-related potentials and fields and early auditory evoked potentials. Additionally, the early auditory wave Pa is modeled by a two-dimensional dynamical system. The segmentation method detects ERP- and ERF-components and early auditory waves objectively, which illustrates the independence of the segmentation method from the number of segments. Additionally, we find a common topology of wave Pa, which indicates a common underlying attractor in the brain.

## 1 Introduction

In neuroscience, multivariate time series are measured at different spatial and temporal scales. Experimental paradigms, which focus on temporal aspects of brain signals, apply frequently, electroencephalography (EEG) or magentoencephalography (MEG) for data acquisition. Data analysis techniques for EEG are based on assumptions about statistical properties of signals or underlying dynamics. Especially models for multivariate signals lead to improved analysis and a better understanding of underlying processes.

The top-down approach aims at extracting models from measured data. For instance, it comprises methods attacking ill-posed inverse problems and modeling of multivariate frequency spectra. Several works have developed segmentation methods, which detect quasi-stationary spatio-temporal states in EEG [Brandeis et al., 1995], [Lehmann & Skrandies, 1980]. [Flexer & Bauer., 1998], [Wackermann, 1999]. These states are supposed to represent coherent neural activities and are called *microstates* [Lehmann & Skrandies,

1980, [Pal et al., 1985]. The work of Lehmann and Skrandies [1980] represents one of the first methods in this field. Starting from the assumption, that coherent neural activity is reflected by global maximum power of EEG, a Global Field Power(GFP) is computed as the root mean square of potential deviations from the spatial average. This definition retains GFP independent of the applied reference electrode. Since coherent states are observed quasistationary in time, transitions between states show changing spatial patterns at short time scales. That is, borders of coherent states are marked by an increased dissimilarity of consecutive spatial activities. This aspect leads to the definition of a Global Dissimilarity (GD). It is computed by the GFP of potential differences of consecutive intensity maps, which are normalized with respect to their GFP [Lehmann, 1992]. Plotting GFP and GD with respect to time, peaks of GD coincide with troughs of GFP. The corresponding time points mark borders of coherent states, i.e. global dissimilarities of intensity maps show least global intensity of EEG. These segmented time windows are called microstates and show one prominent peak of GFP. Comparisons of microstates in ERP-data with well-known cognitive components show good accordance [Brandeis et al., 1995]. An extension of the method has been developed by Pascual-Marqui et al. [1995] by introducing a clustering approach. Here, clusters in multivariate signals are detected by the K-Means algorithm, while the number of clusters are estimated by cross-validation. The present work aims to extent these methods by an additional feature. We introduce and apply a novel clustering approach [Hutt et al., 2001], [Hutt, 2002], which moves the problem of the right number of clusters to a simple statistical problem.

As a second step, multivariate signals are modeled by low-dimensional dynamical systems. The applied method fits optimal projection modes and deterministic ordinary differential equations synchronously. The optimal choice of both modes and dynamical systems have been studied in several works [Kirby, 1992], [Uhl et al., 1993], [Jirsa, 1995], [Kwasniok, 1996], [Ramsay, 1997], [Uhl & Friedrich, 1999], [Hutt et al., 1999]. The present work applies Dynamical Systems Based Modeling(DSBM) [Uhl et al., 2001] based on an analytical treatment [Hutt et al., 1999].

Applications of clustering and DSBM to event-related potentials (ERP), event-related fields (ERF) and middle-latent auditory evoked potentials (MAEP) allows the objective extraction of functional components. Modeling of MAEP-component Pa yields a common topology, which may represent an underlying attractor of component Pa.

The paper is organized as follows. In Sec. 2., we introduce the clustering method and DSBM. The subsequent section contains clustering results obtained from ERP, ERF and MAEP-data. Results are discussed in Sec. 4, which also contains a short outlook.

# 2 Basic Concept

In the present work, we aim at clustering a multivariate signal to obtain temporal segments. Corresponding to previous results [Hutt et al., 2000], quasi-stationary signal parts result from metastable attractors in data space. These attractors generate clusters in data space. Hence, detecting attractors in high-dimensional data space can be done by clustering signal data, where clusters define attractive regions in data space [Hutt et al., 1999]. We apply the K-Means-algorithm [Duda & Hart, 1973] for clustering, but any other unsupervised clustering algorithm is possible (e.g. [Duda & Hart, 1973], [Fränti et al., 1997], [Kundu, 1999]). In a first step, Euclidean distances of each data point to cluster centers are computed. Plots of distances with respect to time illustrate the multi-dimensional structure and temporal behaviour of data points. Small distances from data points to cluster centers indicate attracted data points, while large distances reflect no attractions. We point out, that little clusters, which contain only few data points, are regarded less reliable than large clusters. While clusters of few points might emerge by chance from numerical artifacts or reflect outliers in the data, large clusters originate presumably from real data clusters. This notion of reliability is introduced as each data point is member of one cluster by definition. The average percental contribution of each data point to the clustered structure, or in other words, the reliability of clustered data points, is expressed by a cluster quality measure p(i) [Hutt & Kruggel, 2001]. The average is computed by summation of cluster results obtained from different number of clusters. Good convergence of results is achieved for averages of 30 cluster results.

The obtained cluster quality measure p(i) represents a kind of probability, that a data point i is part of a reliable cluster. The smaller p(i), the higher the probability that i belongs to outliers or parts between clusters. Dropoffs and sharp rises with increasing time indicate final and initial borders of clustered points, respectively. Hence, alternating drop-offs and rises indicate temporal segments of clustered points i.e. regions of attractors.

Figure 1: Kanizsa-figures presented in the visualization task experiment. The square-figure (left) represented the target.

Focusing to data segments of attractors, we aim at modeling dynamics of the signal by its projecting to few spatial modes and synchronous fit of ordinary differential equations. The method minimizes a cost function

$$V = V_s(\mathbf{w}_i, \mathbf{w}_i^{\dagger}) + \epsilon \cdot V_d(\dot{\mathbf{q}}\mathbf{w}_i^{\dagger} - f_i) \quad , \quad \epsilon \in \Re_0^+,$$

which contains one term  $V_s$  for optimal spatial modes and one term  $V_d$  for the dynamics fit. Optimal biorthogonal projection modes  $\mathbf{w}_i, \mathbf{w}_j^{\dagger}$  and corresponding dynamical systems  $f_i$  are obtained for a fixed number of dimensions. Dimensionality effects and a criterion for the optimal weighting  $\epsilon$  have been investigated and derived in [Hutt et al., 1999], [Hutt & Riedel, 2002], respectively.

# 3 Applications

# 3.1 Event-related potentials and fields

This section presents clustering results, which are obtained from ERP- and ERF-data of two similar visual experiments [Herrmann et al., 1999], [Herrmann & Mecklinger, 2000]. In both cases, the stimuli consist of two Kanizsa-figures and two non-Kanizsa figures (Fig. 1) with equal probability of appearence p=0.25. In the ERP-experiment [Herrmann et al., 1999], subjects had to count silently the occurence of Kanizsa-square figures. In the twin experiment [Herrmann & Mecklinger, 2000], which acquired event-related fields, a button had to be pressed at the appearence of the Kanizsa-square figure. In both studies, 10 subjects were shown 400 stimuli in 4 blocks with a duration of 700ms and random interstimuls-intervals between 1000ms and 1500ms.

The EEG was recorded with 64 electrodes at a temporal sampling rate of

Figure 2: Sampled time series of potential maps of ERP-data.

500Hz and filtered with a 0.05Hz high pass and 100Hz low pass-filter. After artifact rejections, the data was averaged over trials and subjects between 200ms before and 900ms after stimuls onset.

MEG-data was obtained by 148 channels at a temporal sampling rate of 678Hz and high pass-filters at 0.1Hz and low pass-filters at 200Hz. As the EEG-data, trials and subjects were averaged between 200ms before and 900ms after stimuls onset. Figures 2 and 3 show sampled time series of maps of the ERP- and ERF-data, respectively.

In Fig. 4, Euclidean distances of ERP-data are plotted for several number of clusters. For K=2 (top row, left side), we observe that the signal evolves near one cluster center (black curve), while it is far from the other cluster center (red curve). At  $\sim$  180ms, the signal leaves the vicinty of the first cluster center and moves to the second cluster. We observe this change of clusters by the smaller distance from data to the second cluster center. At  $\sim$  520ms, the signal changes back to the first cluster. Since results strongly depend on the number of detected clusters, we compute Euclidean distances for several numbers of clusters K. Increasing K, convergence of time points of cluster changes is observed. For K=6 and K=7, cluster results show similar cluster borders at  $t_1\approx 60$ ms,  $t_2\approx 110$ ms,  $t_3\approx 170$ ms,  $t_4\approx 320$ ms and  $t_5\approx 470$ ms. There is one additional change of clusters at 210ms for

Figure 3: Sampled time series of field maps of ERF-data.

Figure 4: Euclidean distances plotted with respect to time for several number of clusters K. In each box, the lowest curve represents the Euclidean distance to the approached cluster.

K=7. In order to obtain a measure, which is independent from the number of clusters, p(t) is computed (Fig. 5). We observe sharp rises and drop-offs of values, which mark initial and final time points of clusters, respectively. Plateaus of values between borders represent constant cluster reliability of points i.e. regions of reliable clusters.

In the following, we introduce clustered windows as windows, which exhibit plateaus of p. Comparing these with known cognitive components, clustered windows V to II mark cognitive components P1, N1, P2 and P3, respectively. The last clustered window I originates from the turn on-off of the visual stimulus. Since cognitive components are defined by latency, polarity and map topology, we compute spatial maps corresponding to clustered windows. These are shown in Fig. 6. Euclidean distances for K=6 and maps of cluster centers are shown in the top and middle row, respectively. Maps of cluster centers are plotted in the sequence of temporal occurrence from left to right. Comparison of cluster centers and well-known components ex-

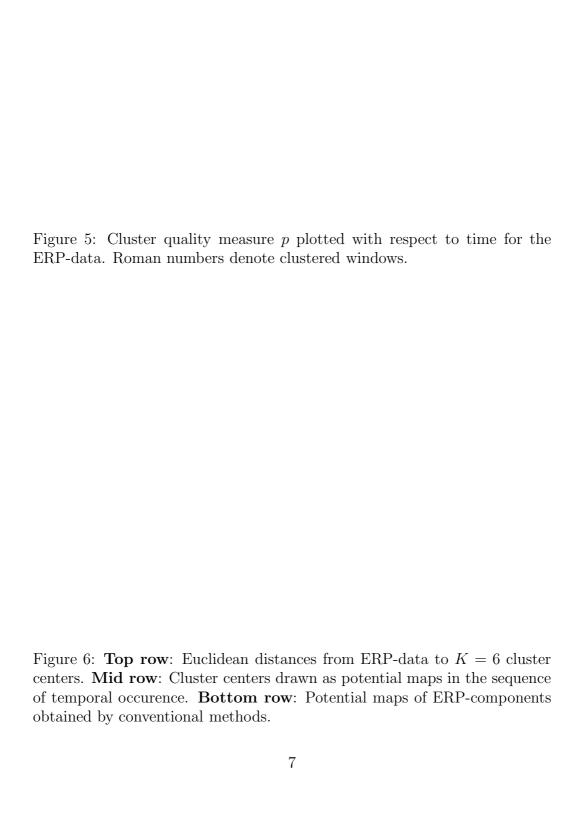


Figure 7: The substructure of component P3. **Top**: Cluster quality measures show three clustered window, while the right most window is least reliable. **Bottom**: Potential maps of corresponding clustered windows.

tracted by conventional methods [Picton et al., 1974] show good accordance of map topology. Hence, clustered windows represent time windows of cognitive components.

Focusing to clustered window II(Fig. 5) and re-applying the clustering method, we observe a substructure (Fig. 7). Hence, component P3 appears to show three, presumably overlapping, additional components in different time windows. We point out, that we are aware of the low reliability of this interpretation from clustering results, as the observed data represents averaged data over subjects. It is well-known, that single subjects show latency shifts of cognitive components, which lead to smeared averaged components. However, we point at the method property of resolving subtle structures in data. Examinations of single-subject data are in progress.

Now, we apply the clustering approach to ERF-data. In Fig. 8, computed cluster quality measures p are plotted with respect to time. We observe sharp rises, plateaus and drop-offs of p. Distinguished clustered windows are detected in time windows [106ms; 134ms], [152ms; 182ms], [191ms; 320ms] and [430ms; 560ms]. Figure 9 shows Euclidean distances for K = 6 (top row) and corresponding maps of cluster centers(middle row) in sequence of temporal

occurrence. The comparison of maps with results obtained by conventional methods (bottom row) show very good accordance and we identify components P1m, N2m, P2m and P3m.

The previous examinations present the clustering method as an objective detection algorithm for quasi-stationary states in ERP- and ERF-data. In the following section, clustering is applied to early auditory evoked potentials and low-dimensional dynamical models are obtained.

### 3.2 Middle latent auditory evoked potentials

The investigated data sets were obtained from a study in which auditory brain stem responses (ABR) and auditory evoked potentials of middle latency (MAEP) were investigated simultaneously. Stimuli were diotic clicks of 100  $\mu$ s duration. The interstimulus interval was chosen to vary randomly and equally distributed between 62 and 72 ms, yielding an average stimulation rate of approximately 15 Hz. The EEG was recorded with 32 electrodes which were placed according to an extended 10-20-system and Cz served as common reference electrode.

Before digitization, raw data were passed through an analogue anti-aliasing lowpass filter with a cutoff frequency 2 kHz. Data were sampled at a rate of 10 kHz, the recording interval comprised 600 samples in the time interval from -15 to 45 ms relative to stimulus onset. 10000 single trials were recorded and stored to hard disk for offline analysis. They were filtered by a zero-phase forward-backward bandpass filter with corner frequencies 20Hz and 300Hz. The present work analyzes three data sets from different subjects showing low (subject dj), middle (hr) and higher (rh) noise levels. Figures 10, 11 and 12 show the electric activity measured on the scalp for the three subjects. Single channel plots illustrate the temporal dynamics, while the temporal sequences of spatial activities exhibit the spatio-temporal dynamics.

Figure 13 shows the cluster quality measure p plotted with respect to time. At 5 ms, descents in p are observed in all data sets followed by a sharp rise. Following plateaus last until 7 ms, when p drops again. As in the previous chapter, this structure indicates a data cluster in the corresponding time interval. Clusters also are found around 17 ms and 30 ms for all data sets. Latencies of the detected clustered windows show good accordance to known waves V, Na and Pa.

Re-applying the cluster method to cropped time intervals at 30 ms confirms these findings (Fig. 14). The corresponding maps on the left hand side repre-

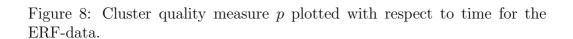


Figure 9: **Top row**: Euclidean distances from ERF-data to K=6 cluster centers. **Mid row**: Cluster centers drawn as field maps in the sequence of temporal occurrence. **Bottom row**: Potential fields of ERF-components obtained by conventional methods.

Figure 10: Measured electric potentials of subject dj. The top plots show activities in the single channels, at the bottom a time series of spatial distributions are shown.

Figure 11: Measured electric potentials of subject hr shown in single channels and as a time series of spatial maps.

Figure 12: Measured electric potentials of subject rh shown in single channels and as a time series of spatial maps.

Figure 13: Cluster quality measure p plotted with respect to time for MAEP-data. Clustered windows are recognized at 5ms (wave V), 18ms (wave Na) and 30ms (wave Pa). The stimulus sets on at 0ms.

sent signal averages over plateaus. They confirm clustered windows by good agreement to quasi-stationary states in the data.

In a next step, DSBM is applied to the clustered window at 30 ms for all datasets. The segment is chosen according to cluster borders in Fig. 14. In a first step, Principal Component Analysis is applied in order to reduce the signal dimensionality with errors  $E < 10^{-5}$  for five modes. These projections serve as a new five-dimensional signal, which is modelled by DSBM.

Two-dimensional projection planes are obtained for each data set from the first two PCA-modes ( $E < 10^{-2}$ ). Synchronously determined dynamical systems are fitted with minimal errors  $V_d(\epsilon = 0.09) = 4 \cdot 10^{-4}$  (data set dj),  $V_d(\epsilon = 0.0) = 4 \cdot 10^{-4}$  (data set hr) and  $V_d(\epsilon = 0.15) = 4 \cdot 10^{-3}$  (data set rh) while applying polynoms of third order. Lower polynomial orders lead to worse fits and bad reconstruction of the signal, whereas higher orders do not lead to new dynamical properties.

The basic assumption of attractors is verified by the topology of obtained dynamical systems. Integrations of obtained differential equations with various initial points leads to sets of trajectories and elucidate the topology of the temporal dynamics (Fig. 15). All data sets show a saddle node FP3 at

Figure 14: Cluster results in time windows of wave  $P_a$ . Window borders are obtained from Fig. 13. Vertical dashed lines mark cluster borders. On the left hand side, averaged spatial distribution in intervals [28.0 ms; 31.0 ms] (dataset dj), [28.0 ms; 31.0 ms] (dataset hr) and [26.6 ms; 30.4 ms] are shown.

y = 0, a stable focus FP4 and another saddle node FP1. The additional stable focus FP2 is detected only in datasets dj and hr.

### 4 Discussion

Let us summarize the results. Figure 5 shows the cluster quality p for ERP-data plotted with respect to time. Since quasi-stationary signal maps represent clusters in data space and time windows of constant values of p indicate clustered data, plateaus I to V represent quasi-stationary maps. These results are independent from the number of clusters and illustrate the objectiveness

Figure 15: Sets of trajectories of component  $P_a$  for all subjects. The right hand side show focused plots of attractive areas on the left hand side. Circles mark initial values of integration, while boxes denote fixed points.

of the proposed cluster method. Corresponding to Fig. 6, detected clusters agree to known cognitive components. Similar cluster results are found in ERF-data. Here, we also find distinguished plateaus of p (Fig. 8), which show good accordance to known ERF-components (Fig. 9).

Finally, we examine early evoked potentials. Cluster applications yield cluster quality measures, which show sharp rises, drop-offs and plateaus (Fig. 13). The observed clustered windows show good accordance to quasi-stationary maps in Figs. 10-12 and early waves V, Na and Pa [Regan, 1989]. Focusing to a time window at wave Pa and re-applying clustering, we gain drop-offs, rises and plateaus at the same time points (Fig. 14). Corresponding spatial maps agree with quasi-stationary patterns in Figs. 10-12.

Applications of DSBM to wave Pa yields optimal projective spatial modes and corresponding amplitudes, which obey dynamical systems. Their corresponding phaseportraits are shown in Fig. 15. We observe a common topology of the dynamics for all subjects.

The proposed two-step analytical framework yields common topologies of component Pa and we conjecture common dynamical attractors as the basic mechanism of the underlying processes in the brain. Relations of neuronal processes and detected fixed points can not be defined yet in the current stage of analysis. However, we obtain both an outlook to a novel approach for modeling neuronal dynamics based on measured data and indications about underlying neuronal attractors. We believe, that examinations of additional single subject data will foster the proposed findings.

# Acknowledgement

The author is indebted to C.S. Herrmann and H. Riedel for valuable discussions and providing the examined data sets.

- Brandeis D., Lehmann D., Michel C.M. & Mingrone W. [1995], "Mapping Event-Related Brain Potential Microstates to Sentence Endings", *Brain Top.* 8(2), 145-159
- Flexer A. & Bauer H., "Discovery of Common Subsequences in Cognitive Evoked Potentials", in *Principles of Data Mining and Knowledge Discovery*, Second European Symposium, PKDD '98, Proceedings, Lecture Notes in Artificial Intelligence, (eds.) Zytkow Y.J.M & Quafafou M., (Springer-Verlag, Berlin), **1510**, 309-317
- Duda R.O. & Hart P.E. [1973], Pattern Classification and Scene Analysis (Wiley, New York)
- Fränti P., Kivijärvi J., Kaukoranta T. & Nevalainen O. [1997], "Genetic Algorithms for Large-Scale Clustering Problems", *The Computer Journal* **40**(9), 547-554
- Friedrich R. & Uhl C. [1996], "Spatio-temporal analysis of human electroencephalograms: Petit-Mal epilepsy", *Physica D* **98**, 171-182
- Herrmann C.S., Mecklinger A. & Pfeifer E. [1999], "Gamma Response and ERPs in a Visual Classification Task", *Clin. Neurophysiology* **110**, 636-642 Herrmann C.S. & Mecklinger A. [2000], "Magnetoencephalographic responses to illusory figures: Early evoked gamma is affected by processing of stimulus features", *Int. J. Psychophysiol.* **38**(3), 265-281
- Hutt A., Uhl C. & Friedrich R. [1999], "Analysis of spatio-temporal signals: A method based on perturbation theory", *Phys.Rev.E* **60**(2), 1350-1358 Hutt A., Svensen M., Kruggel F. & Friedrich R. [2000], "Detection of fixed points in spatiotemporal signals by a clustering method", *Phys. Rev. E* **61**(5), R4691-R4693
- Hutt A. & Kruggel F [2001], "Fixed Point Analysis: Dynamics of Non-stationary Spatiotemporal Signals", in *Space-time Chaos: Characterization*, Control and Synchronization, (eds.) Boccaletti S., Mancini H.L., Gonzales-Vias W., Burguete J. & Valladares D.L. (World Scientific, Singapore)
- Hutt A., Kruggel F. & Herrmann C.S. [2001], "Automatic Detection of ERP-components and their modelling", *J. Cogn. Neuroscience*, Supplement 85
- Hutt A. & Riedel H. [2002], "Analysis and Modelling of Quasi-stationary Multivariate Time Series and their Application to Middle Latency Auditory Evoked Potentials", submitted
- Hutt A. [2002], "Spatiotemporal Modelling of EEG/MEG", Brain Topography, in press
- Jirsa V.K., Friedrich R. & Haken H. [1995], "Reconstruction of the spatiotemporal dynamics of a human magnetoencephalogram", *Physica D* 89, 100-

Kirby M. [1992], "Minimal Dynamical Systems From PDEs Using Sobolev Eigenfunctions", *Physica D* **57**, 466-475

Kwasniok F. [1996], "The Reduction of Complex Dynamical Systems Using Principal Interacting Patterns", *Phsyica D* **92**, 28-60

Kundu S. [1999], "Gravitational clustering: a new approach based on the spatial distribution of the points", *Pattern Recognition* **32**, 1149-1160

Lehmann D. & Skrandies W. [1980], "Reference-free identification of components of checkerboard-evoked multichannel potential fields", *Electroenceph. clin. Neurophysiol* 48, 609-621

Pal I., Horst A. & Lehmann D. [1985], "EEG segmentation in time using spatial criteria - micro-states and reaction-time", *Electroenceph. Clin. Neurophysiol.* **61**(3), 97

Pascual-Marqui R.D., Michel C.M. & Lehmann D. [1995], "Segmentation of Brain Electrical Activity into Microstates: Model Estimation and Validation", *IEEE Trans. Biomed. Eng.* **42**(7), 658-665

Picton T.W., Hillyard S.A., Krausz H.I. & Galambos R. [1974], "Human auditory evoked potentials. I:Evaluation of components", *Electroenceph. clin. Neurophsyiol.* **36**, 179-190

Ramsay J.O. & Silverman B.W. [1997], Functional Data Analysis (Springer, New York)

Regan D. [1989], Human brain electrophysiology: Evoked potentials and evoked magnetic fields in science and medicine, (Elsevier, New York)

Uhl C., Friedrich R. & Haken H. [1993], "Reconstruction of spatio-temporal signals of complex systems", Z. Phys. B 92, 211-219

Uhl C., Hutt A. & Kruggel F. [2001], "Improvement of Source Localization by Dynamical Systems Based Modelling(DSBM)", *Brain Top.* **13**(2), 219-226

Wackermann J. [1999], "Towards a quantitative characterisation of functional states of the brain: From the non-linear methodology to the global linear description", Int. J. Psychophysiology, **34**, 65-80